4ICEGE Thessaloniki-GREECE 2007

4th International Conference on
Earthquake Geotechnical Engineering
June 25-28, 2007
Paper No. 1445

THE ROLE OF THE AMPLITUDE AND FREQUENCY CONTENT OF THE INPUT GROUND MOTION ON THE ESTIMATION OF DYNAMIC IMPEDANCE FUNCTIONS

Dimitris PITILAKIS [1], Didier CLOUTEAU[2], Arezou MODARESSI[3]

ABSTRACT

This paper provides an insight in the role of the amplitude and frequency content of the input ground motion on the estimation of the dynamic impedance functions. The softening of the soil under strong ground shaking is not taken into account in the dynamic impedance functions, under the assumption of linear elastic soil behavior. However, different input ground shaking results into different nonlinear soil behavior, which may have important effects on the amplitude and shape of the dynamic stiffness and radiation damping coefficients. A simple parametric analysis is performed for a typical footing resting on a halfspace soil profile and subjected to five scaled earthquake records. The dynamic impedance coefficients are estimated with an equivalent linear procedure and compared to the linear elastic case. The dynamic stiffness coefficient is found to decrease in amplitude and become frequency dependent, depending on the frequency content characteristics of the ground motion. The radiation damping is found to be unaffected by the nonlinear soil behavior.

Keywords: dynamic impedance function, equivalent linear, scaled excitation

INTRODUCTION

The importance, as well as the general notion of the foundation dynamic impedance function, is well established in engineering practice, during the past three decades (Veletsos 1971, Veletsos 1973, Gazetas 1983, Dobry1986a, Dobry1986b, Gazetas1991a, Gazetas 1991b, Sieffert 1992, Pecker 1997, Mylonakis 2006). The general equation, extracted from Gazetas 1983,

$$\mathbf{S} = K\,(\,\mathbf{k}(\omega,v) + \imath\,\alpha_0\,\mathbf{c}(\omega,v)\,)\,(1+2\,\imath\,\xi) \tag{1}$$

provides the dynamic impedance function **S** in terms of the static stiffness K, the dynamic stiffness and damping coefficients $\mathbf{k}$ and $\mathbf{c}$ respectively, and the hysteretic material damping ratio ξ of an equivalent SDOF oscillator. The dimensionless parameter

$$\alpha_0 = \omega B/V_s \tag{2}$$

normalizes the excitation frequency ω with a characteristic dimension B of the foundation and the shear wave velocity V_s of the supporting soil.

Geometrical and material linearity is implicit in equation (1). The static stiffness of the footing depends on the initial shear modulus G of the supporting soil and the Poisson's ratio v, while the dynamic stiffness and damping coefficients depend on the excitation frequency. The hysteretic

[1] Civil Engineer, Ph.D., Ecole Centrale Paris, France (Currently at the Department of Civil Engineering, University of Thessaloniki, Greece), Email: dimitris.pitilakis@gmail.com
[2] Professor, Ecole Centrale Paris, France
[3] Professor, Ecole Centrale Paris, France

material damping ξ depends on the initial linear material properties of the soil. Besides, the dimensionless frequency parameter α_0 depends on the shear wave velocity of the linear soil. For convenience and to avoid any misconceptions, the shear wave velocity of the supporting soil will be assumed herein as the shear wave velocity $V_{s,30}$ of the upper 30m of soil, according to the Eurocode 8 (CEN, 2002)

As opposed to the idealization of the linear soil behavior, the dynamic material properties of the soil are not constant when the soil behaves in a nonlinear way. The shear modulus G and, consequently, the shear wave velocity $V_{s,30}$ change in time with varying earthquake excitation amplitude and frequency content. Thus, equation (1) cannot be directly implemented in the nonlinear soil behavior case, since the abovementioned parameters vary. As a result, the foundation dynamic impedance functions have to be calculated in terms of the modified soil-foundation system properties. For that reason, an equivalent linear approach can be implemented in the calculation of the foundation dynamic impedance functions, using equivalent linear shear modulus and damping characteristics.

An equivalent linear procedure is used herein to calculate the dynamic impedance functions of a foundation supported on a soil profile having equivalent linear properties (Pitilakis D., 2006). The soil-foundation system is subjected to five different earthquake ground motions consisting of body waves, propagating only on the vertical direction. The effect of the different ground motion amplitude and frequency content on the dynamic foundation impedance functions is clearly demonstrated.

The computation of the dynamic foundation response is performed assuming that there is no structure founded on the footing. Moreover, the foundation is assumed usually massless in a typical calculation of the dynamic impedance functions. Therefore, no secondary nonlinear effects are expected to appear in the soil, as there is no diffracted wave field, created by the foundation-structure vibration and emanating away from the foundation to infinity. There would still be created a diffracted wave field due to kinematic interaction but it vanishes in the present case for vertical incidence and surface foundations. Assuming that the secondary nonlinearities induced in the soil are approximately zero, the dynamic impedance functions estimated by the equivalent linear procedure can be used for the computation of the SSI with an equivalent linear soil behavior.

SYSTEM IDENTIFICATION

In a linear soil-foundation system, factors that influence the dynamic foundation impedances are identified by several authors. Among them are the foundation shape and flexibility, the embedment ratio, the excitation frequency, the type of soil profile along with the depth and stiffness of the bedrock, the soil properties (shear modulus, Poisson's ratio, hysteretic damping ratio), the soil anisotropy, inhomogeneity and nonlinearity.

In the nonlinear soil-foundation system, however, parameters such as the intensity and frequency content of the signal may modify significantly the response from one case to another, by exciting the nonlinear response of the soil. In contrast with the linear soil case, the nonlinear soil behavior tends to decrease the stiffness of the system and to increase the energy dissipation by viscous and hysteretic mechanisms in the soil. Thus, additional parameters enter in the estimation of the foundation dynamic impedance functions.

In order to reveal the effects of the nonlinear soil behavior, and more specifically of the different input ground motion, on the foundation dynamic impedance functions, a series of parametric analyses is performed. A rigid massless footing is placed a homogeneous halfspace soil profile and is subjected to a harmonic motion. Up to this point the procedure is similar to the largely exploited procedure, assuming linear soil behavior, presented in numerous studies. The nonlinear soil behavior is approximated by shear modulus reduction and damping curves for a typical clayey soil materials, notably clay with IP0. Furthermore, the soil-foundation system is subjected to five different

earthquake records and the response is obtained in the light of the substructure technique with equivalent linear soil properties.

Due to the inherent complexity of such an approach to the equivalent linear dynamic impedance functions, several assumptions have to be made for sake of simplicity and comprehension. Accordingly, the soil-foundation system properties are chosen so as to cover the wider possible range of cases with the minimum number of interfering parameters.

Foundation Identification

The foundation consists of an infinitely rigid, massless circular footing of diameter d=10m, resting on the free soil surface. Any arbitrary shaped footing can be approximated by an equivalent circular one, by equating the contact surfaces for the three translational degrees of freedom and the area moments of inertia for the three rotational components.

The radius of the circular foundation, r=5m, was chosen sufficiently large in order to account for the kinematic interaction, along with the inertial interaction, for a vast range of shear wave velocities and frequencies. The circular footing is meshed in 334 quadrilateral and 4 triangular elements with an average size of 0.5m, as shown in Figure 1.

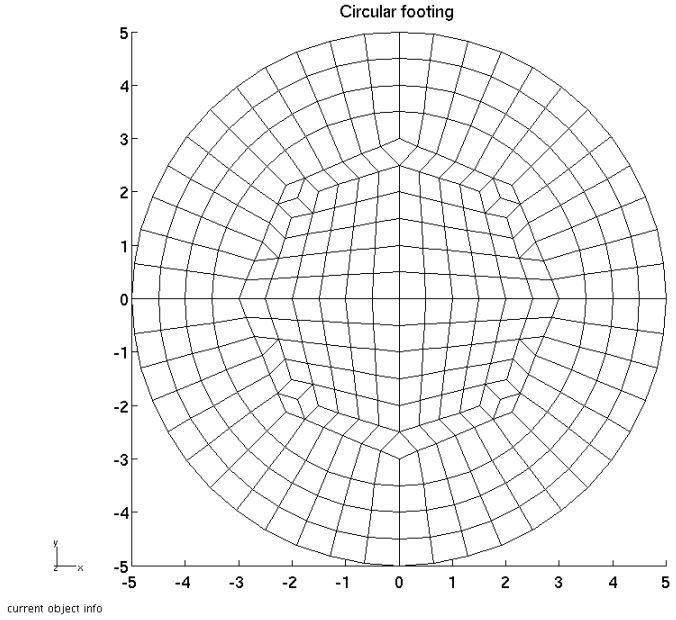

Figure 1. Rigid massless circular footing used in the parametric analyses

Different mesh configurations were tested, using larger or smaller number of elements, different sizes as well as different types of elements. More specifically, configurations were tested using 99 quadrilateral elements, 321 quadrilateral elements, 241 triangular elements, and the chosen configuration of 334 quadrilateral and 4 triangular elements. The real and imaginary parts of the estimated dynamic impedances were compared against the reference solution proposed by Sieffert (1992). The presented configuration (334 quadrilateral and 4 triangular elements with an average size of 0.5m) is chosen based on the accuracy and the time efficiency of the achieved solution.

For a rigid, circular, massless footing resting on a perfectly elastic halfspace, the static stiffness of the circular disk in the horizontal, vertical, rocking and torsional modes are calculated according to Veletsos (1973),

$$K_x = 8Gr / (2-\nu) \quad (3)$$

$$K_z = 4Gr / (1-\nu) \quad (4)$$

$$K_\theta = 8Gr^3/3(1-\nu) \quad (5)$$
$$K_t = 16Gr^3/3 \quad (6)$$

where G and v are the initial shear modulus and Poisson's ratio respectively for the soil, assuming linear conditions, and r is the radius of the footing. The static stiffness of the disk expresses the force which is necessary to produce a unit displacement or rotation, for the two translational and the rotational modes of vibration respectively.

In the vibration of a footing under loading, the amplitude of the dynamic response in each mode depends on the zone of influence, which is the depth to which the normal stresses extend in the soil. Therefore, for a circular footing resting on a homogeneous halfspace, the vertical normal stresses induced along the centerline of the foundation extend to a depth of five radii. For a horizontally loaded footing, the horizontal stresses induced in the soil vanish at depth larger than two radii, while for moment and torsional loading the stresses practically exist down to a depth of 1.25 and 0.75 radii respectively (Gazetas 1983).

Soil Profile Identification

The footing is placed on the free surface of a homogeneous soil profile, as shown in Figure 2. For convenience, the thickness of the soil stratum is chosen equal to H=30m. For the homogeneous halfspace shown in Figure 2, five different shear wave velocities $V_{s,30}$ are assigned, notably 100m/s, 180m/s, 250m/s, 350m/s, 500m/s, classifying the soil profile to category types C and B according to the Eurocode 8.

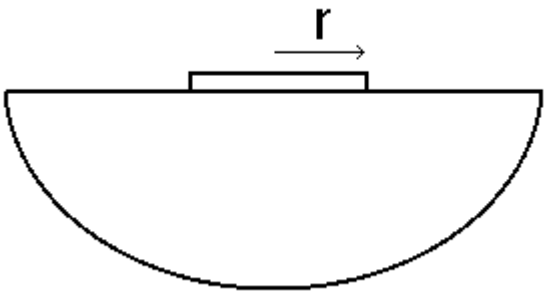

Figure 2. Homogeneous halfspace soil profile supporting the circular footing

In order to approximate the nonlinear behavior of the soil with an equivalent linear approach, a clay with plasticity index IP0, according to Vucetic (1991), is used to describe the clayey soil material (Figure 3). This curve is widely used in engineering practice and describes a typical clayey soil material.

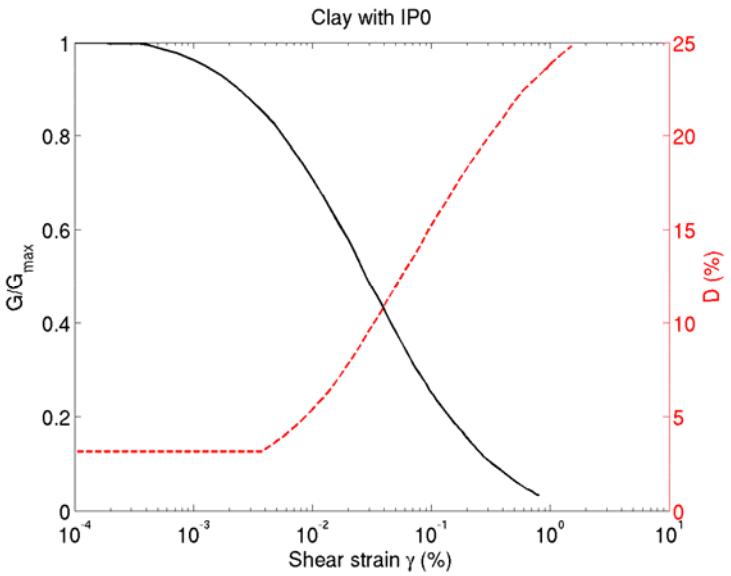

Figure 3. Shear modulus reduction and damping curves for the clay IP0 soil material

A discretization of the soil profile in soil layers is performed, in order to calculate the shear strain level at different depths and vary the shear modulus and the damping accordingly. Therefore, the soil profile of 30m is divided into five layers, having thickness from top to bottom of 1m, 2m, 4m, 8m and 15m. The soil profile in all the analyses has a typical unit weight of 2000kg/m^3. Moreover, even though in most of the available literature on the foundation impedance functions zero material damping is assumed in the soil, it is confirmed that even at small strain levels the soil behaves in a hysteretic way (Dobry 1986a, Dobry 1986b). The latter is more pronounced, naturally, in the case of a nonlinear soil behavior and thus, an initial hysteretic damping ratio is set at 2% for linear soil conditions. The Poisson's ratio is set at 1/3, a typical value for unsaturated soil.

Ground Motion Identification

In order to promote the nonlinear soil behavior, the soil--foundation system is subjected to five earthquake records, chosen according to the European tectonic environment, with varying amplitude and frequency content. The five earthquake records are notably the Aegion, 1995 Aegion, Greece earthquake record, the Bucharest, 1977 Bucharest, Romania earthquake record, he San Rocco, 1976 Friuli, Italy earthquake record, the Kozani, 1995 Kozani, Greece earthquake record and the Umbria, 1984 Umbria, Italy earthquake record. The five earthquake records are scaled to maximum acceleration amplitude of 0.01g, 0.10g, 0.20g, 0.30g and 0.50g, in order to cover a wide range of ground motion amplitudes. However, one must keep in mind that scaling an accelerogram might affect and indeed modify its frequency content. Nonetheless, in the parametric analyses conducted the frequency content of the input ground motions is not as important parameter for the nonlinear soil behavior as the excitation amplitude. For acceleration amplitude 0.01g, the soil is expected to behave in a linear way. The five earthquake ground motions are chosen so that a wide range of excitation frequencies is covered. Furthermore, the five earthquake records cover a wide range of response spectrum natural periods. Figure 4 shows the response spectra of the five unscaled earthquake records and Figure 5 shows the their Fourier spectra. The five earthquake records vary from very low frequency content, such as the Bucharest earthquake record, to high frequency records as the Umbria earthquake record.

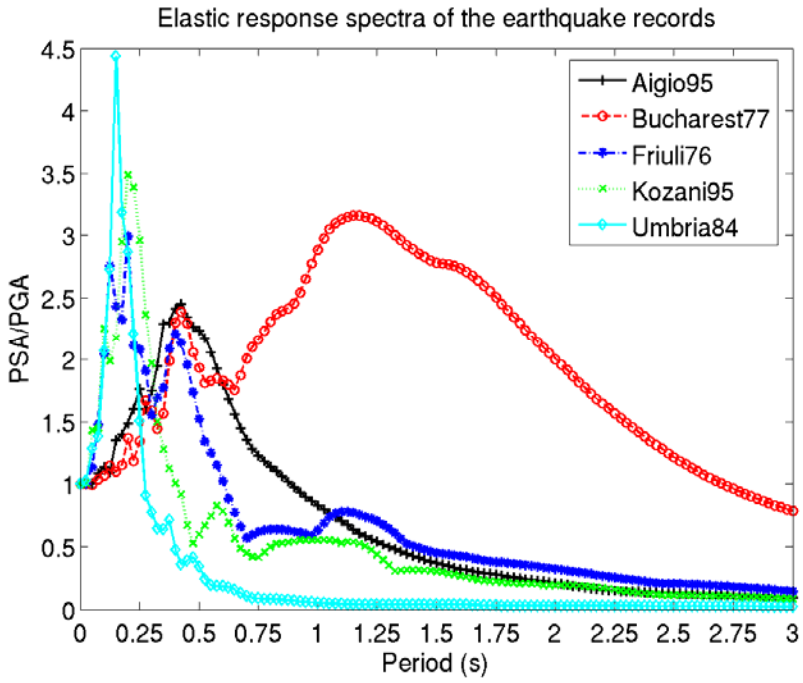

Figure 4. Elastic response spectra of the five earthquake ground motions

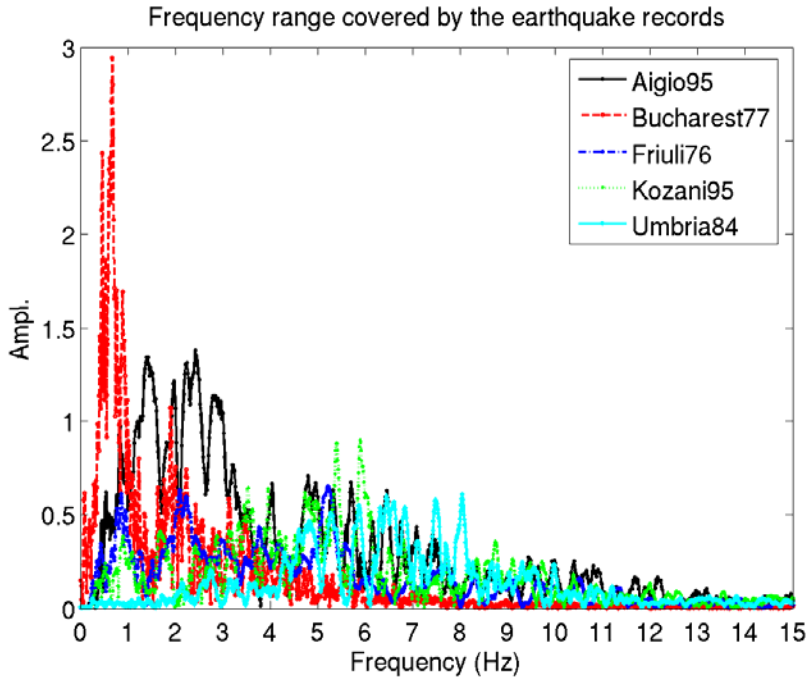

Figure 5. The Fourier spectra of the five unscaled earthquake records show the frequency range covered by the parametric analyses

Thus, using five earthquake records with significantly different frequency content and scaled amplitudes covers sufficiently a wide range of earthquake scenarios with scattered amplitudes and frequency contents.

PARAMETRIC ANALYSES

A parametric analysis is performed in order to investigate the effects of the nonlinear behavior of the soil on the dynamic foundation impedance functions. The analyses of soil--foundation systems comprise a halfspace soil profile of a typical clay, five initial shear wave velocities for the profile (100m/s,180m/s, 250m/s, 350m/s, 500m/s), and five earthquake records scaled to five different amplitudes.

In the simple linear case the foundation dynamic impedance function are affected primarily by the parameters mentioned in a previous section. Thus, it is immediately understood that the complexity of the problem increases in the nonlinear soil case as the number of the parameters that influence the soil response increase.

As the typical procedure for calculating the dynamic impedances of a footing suggests (equation (1)), the static stiffness is calculated from equations (3) to (6) and the dynamic stiffness and damping coefficients are estimated from normalized graphs and charts. An attempt is made to estimate such dimensionless graphs for the equivalent dynamic stiffness and dashpot coefficients. Then, knowing the dynamic impedance coefficients of the footing, the response of the superstructure can be calculated from standard rigid body dynamics.

Four components of the circular footing vibration are examined, notably the horizontal, vertical, rocking and torsional. The real part of the dynamic impedance in equation (1), namely the dynamic stiffness coefficients are noted by k_x , k_z , k_θ and k_t respectively, while the imaginary part of equation (1) expresses the radiation damping coefficients, which are denoted by c_x, c_z, c_r and c_t, respectively. Both the real and imaginary parts of the impedances are always normalized by the linear static stiffness for the corresponding mode of vibration, presented in equations (3) to (6). For the real part of the dynamic impedance, the dynamic stiffness coefficient, the dimensionless frequency parameter, notably $\alpha_0 = \omega B/V_{s,30,LIN}$ in a linear analysis, is enriched by a correction factor of $V_{s,30,LIN}/ V_{s,30,EQL}$ in order to include the effect of the soil softening due to nonlinear behavior. The correction factor $V_{s,30,LIN}/ V_{s,30,EQL}$ is indeed the ratio of the initial, linear shear wave velocity assigned to the soil profile over the shear wave velocity calculated for the soil profile having equivalent linear characteristics. Attention should be made, as will be seen, in reading the charts, as the equivalent linear shear wave velocity differs in each soil case, depending on the properties of the soil and the dynamic characteristics of the input signal. From a practical point of view, multiplying the dimensionless α_0 parameter by $V_{s,30,LIN}/ V_{s,30,EQL}$ moves the dynamic stiffness coefficient impedance curve to the right, i.e. to the higher frequency range. Nevertheless, this horizontal translation to the higher frequency range is the counterpart of the shifting of the dynamic stiffness coefficient to the lower frequency range, due to the soil softening. The result is the canceling of the shifting to the lower and to the higher frequency range, that is the peak response will appear at the same position as it appears in the linear case.

Contrary to the dynamic stiffness coefficient k, the imaginary part of the dynamic impedance, namely the radiation dashpot coefficient c times the dimensionless parameter α_0, $\alpha_0\, c$, is plotted against α_0 without any normalization. The imaginary part is plotted in its integrity ($\alpha_0\, c$), instead of c, in order to avoid divergence at low frequencies. For sake of simplicity, the imaginary part of the dynamic impedance $\alpha_0\, c$, will be referred to herein simply as radiation dashpot coefficient.

Effect of Different Input Ground Motion

The same soil profile subjected to different earthquake ground motions will respond differently, according to the input ground motion dynamic characteristics and more accurately on the amplitude and on the frequency content. Hence, the same soil-foundation system, when the nonlinear soil behavior is approximated with an equivalent approach, may also respond in a different way to two different earthquake ground motions.

For the purpose of showing that different behavior, the soil-foundation system comprising of the circular footing resting on the surface of a homogeneous halfspace of clayey soil with IP 0 and having initial shear wave velocity $V_{s,30}$ =180m/s is first subjected to the scaled Aegion, 1995 Aegion, Greece earthquake record. Figure 6 to Figure 9 show the horizontal, vertical, rocking and torsional dynamic impedance coefficients respectively.

The horizontal dynamic stiffness coefficient decreases from the linear case in amplitude with increasing level of excitation amplitude (Figure 6). The fluctuations in the stiffness coefficient curves are the apparent result of resonances that occur in the soil. The initially homogeneous halfspace soil profile behaves in a nonlinear way and interfaces are formed in the soil between layers with different impedance ratios. Consequently, waves emanating from the vibrating foundation are reflected on those interfaces and propagate back towards the footing. The result of this propagation is the increase of the foundation motion in some frequencies, close to the resonance frequencies of the newly formed inhomogeneous soil. The short and flat peaks imply no significant impedance ratio between the formed soil layers, whereas they appear in the resonant frequencies of the soil.

Contrary to the linear case, in the lower frequency range the magnitude of the dynamic impedance stiffness increases with increasing frequency, attains a peak and then decreases following the trend of the linear case, showing certain frequency dependence. This contradictory behavior in the low frequency range (dominated by the response of the deeper soil layers to low frequency, large wave length, pulses) is caused by an inversion of the shear wave velocity with depth. For an earthquake amplitude of 0.30g, the shear wave velocity decreases with increasing depth. At a depth of 11m, the shear wave velocity is 77m/s, while it is 171m/s at a depth of 0.5m under the foundation. Similarly, the shear modulus reduces down to 10% of the maximum linear elastic value G_{max}. Thus, the low frequency response is dominated by pulses propagating at significantly lower shear wave velocities than the initial linear case, resulting in a stiffness coefficient significantly decreased in amplitude from the linear case. On the other hand, in the high frequency range the response is dominated by the surface waves which are allowed to be created. These waves propagate in a higher shear wave velocity, with a shorter wavelength, than the low frequency deeper body waves, leading to a increase in the dynamic stiffness of the footing in the higher frequency range. In conclusion, the increase of the dynamic stiffness coefficient with increasing frequency is due to the decrease of the shear wave velocity with increasing depth, after the equivalent linear analysis. In the case of Figure 6, the decrease of the stiffness in the high frequency range, after the peak, is caused by an eventual increase of the shear wave velocity, computed to be 83m/s at a depth of 22.5m (from 77m/s at 11m depth).

The imaginary part of the dynamic impedance, plotted in Figure 6, is the combined effect of the radiation viscous damping and the hysteretic material damping. Assuming a purely elastic soil, if there were no hysteretic damping in the equivalent linear analyses, the values of the imaginary part of the dynamic impedance would be zero, implying that the radiation dashpot would be zero. On that account, the non zero value of the radiation dashpot for zero frequency, even for the linear case, denotes the presence of the hysteretic damping (equal to 2% in the linear analyses). In the linear case, the imaginary part increases at a constant rate with increasing frequency, implying that the radiation damping is practically independent of the frequency. In the equivalent linear case, the magnitude of the imaginary part of the impedance increases from the linear case with increasing excitation amplitude. This increase is attributed primarily to the hysteretic material damping of the soil, which indeed increases in the equivalent linear soil with increasing level of excitation. For an earthquake amplitude of 0.30g, the hysteretic damping increases up to 17% in the deeper soil layers. The radiation viscous damping in the horizontal mode increases with increasing frequency at the same rate as in the linear case. This explains the fact that the radiation dashpot coefficients are transposed in parallel from the linear case, apparently unaffected by the soil nonlinearity. For the nonlinear case, the larger the excitation amplitude, the larger the parallel transpose of the curve to higher values.

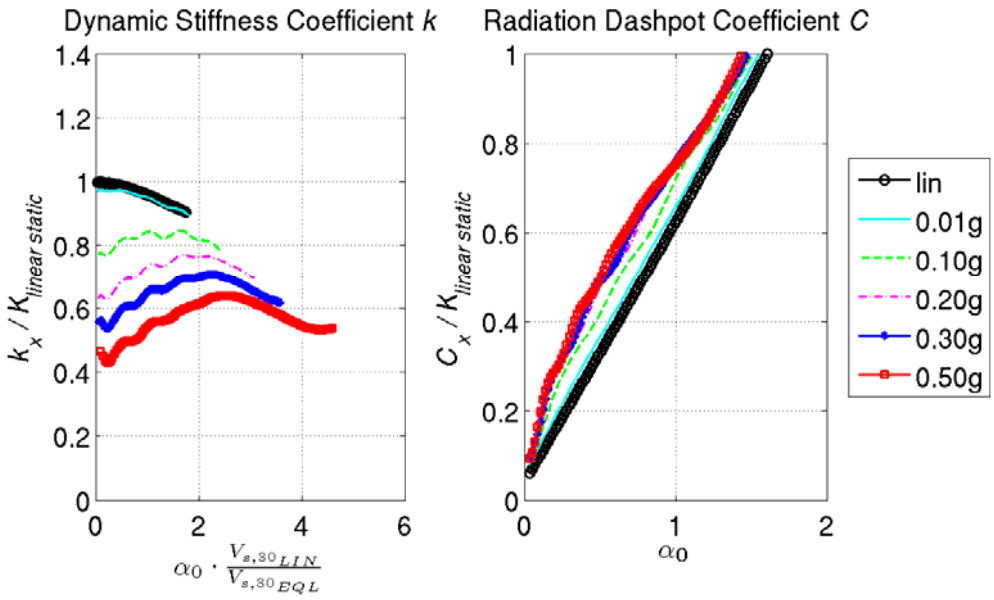

Figure 6. Horizontal dynamic stiffness and radiation dashpot coefficients for a homogeneous soil profile, with clay IP0 soil, initial shear wave velocity $V_{s,30,LIN}$=180m/s, subjected to the Aegion earthquake record

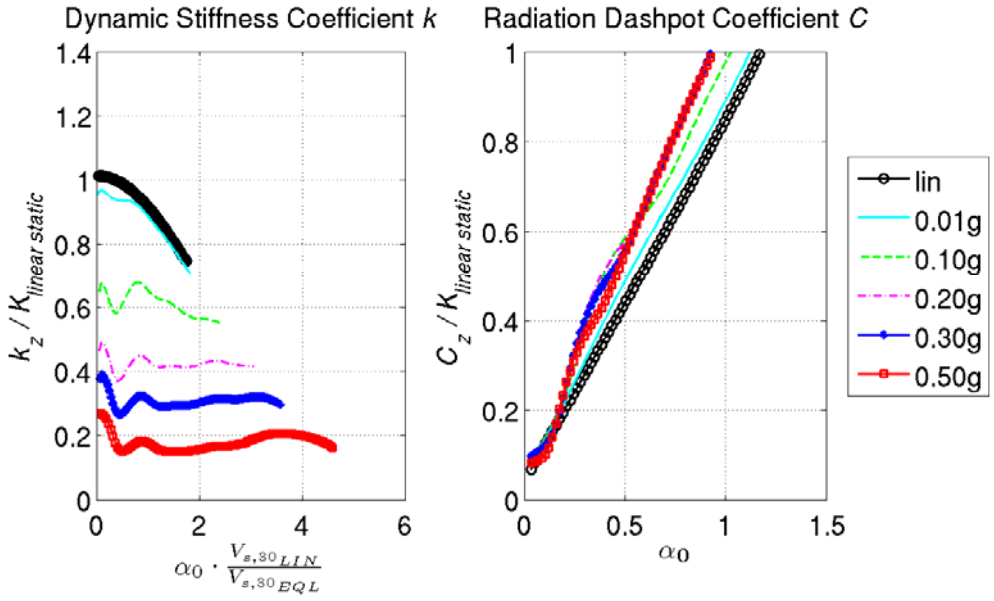

Figure 7. Vertical dynamic stiffness and radiation dashpot coefficients for a homogeneous soil profile, with clay IP0 soil, initial shear wave velocity $V_{s,30,LIN}$=180m/s, subjected to the Aegion earthquake record

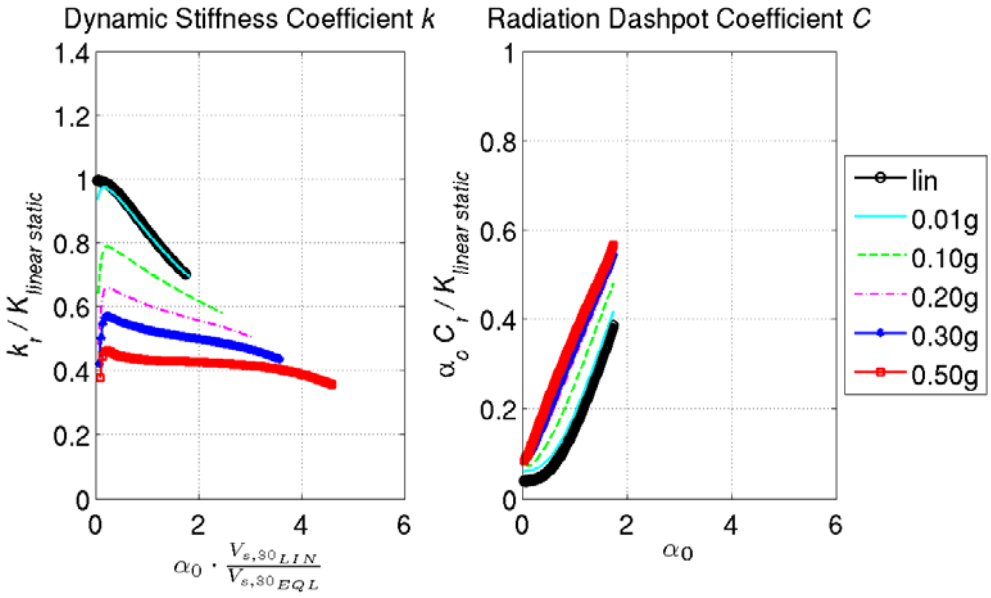

Figure 8. Rocking dynamic stiffness and radiation dashpot coefficients for a homogeneous soil profile, with clay IP0 soil, initial shear wave velocity $V_{s,30,LIN}$=180m/s, subjected to the Aegion earthquake record

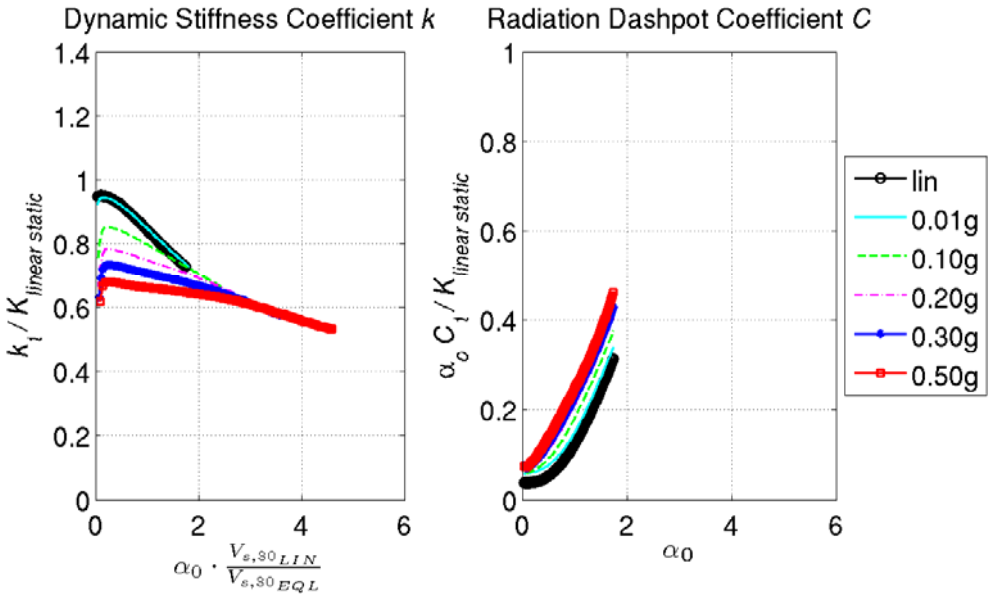

Figure 9. Torsional dynamic stiffness and radiation dashpot coefficients for a homogeneous soil profile, with clay IP0 soil, initial shear wave velocity $V_{s,30,LIN}$=180m/s, subjected to the Aegion earthquake record

In the low frequency range, however, the hysteretic damping in the equivalent linear analyses does not increase from the linear case, causing the radiation dashpot coefficient curves for all excitation amplitudes to be similar in amplitude with the linear case. This arises from the fact that in the low frequency range no surface waves are created. The response of the soil is dominated by the wave fields having longer wave lengths, which create resonance phenomena at larger depths. As in the equivalent linear analysis the halfspace soil profile is discretized into soil layers with refined thicknesses closer to the surface, the increase of the hysteretic material damping is taken into account mainly in the upper soil layers and not in the deeper. Thereby, the predominant low frequency waves in the deeper soil layers do not influence the equivalent linear soil response, resulting in a minor increase of the hysteretic damping from the linear case.

The effects of the soil softening due to nonlinear behavior are more pronounced in the vertical stiffness coefficient in Figure 7. This is expected because of the deeper zone of influence of the vertical normal stresses in the soil, caused by the vertical loading of the footing. The magnitude of k_z decreases with increasing excitation amplitude, reaching a reduction of 80% for the case of the excitation amplitude 0.50g. Furthermore, the nonlinear soil is not homogeneous any more, as seen from the peaks and valleys for values of the dimensionless frequency parameter $\alpha_0\ c\ V_{s,30,LIN}/\ V_{s,30,EQL}$ less than 1. The location of the resonant valleys coincides with the resonant frequencies of the soil.

Concerning the vertical radiation dashpot coefficient, the increase in the hysteretic damping with increasing excitation amplitude, in the medium to higher frequency range, is apparent in the vertical mode as well. The low frequency range is dominated by the effects of the deeper soil layers, in which the increase in hysteretic damping is not accounted in the equivalent linear analysis. The radiation damping coefficient in the vertical mode is slightly affected by the increase of amplitude, increasing with frequency with a bit larger rate than in the linear case.

Similar trends are observed in the rocking (Figure 8) and torsional (Figure 9) vibration modes equally. The stiffness decreases from the linear case with increasing excitation amplitude, while it tends to become frequency independent with increasing level of excitation amplitude. The hysteretic damping increases with increasing excitation amplitude while the radiation damping is unaffected by that increase. The radiation damping for the nonlinear cases increases with frequency at the same rate as in the linear case. The small, compared to the translational modes, radiation coefficient values attested by researchers for the rocking and torsional modes, are confirmed for the nonlinear case as well. Yet, the radiation damping coefficients are at least 50% lower than they are for the translational components.

Next the same soil-foundation configuration is subjected to the San Rocco, 1976 Friuli, Italy earthquake record. The horizontal, vertical, rocking and torsional dynamic impedance coefficients are shown in Figures 10 to 13 respectively.

In the horizontal response (Figure 10) the dynamic stiffness decreases from the linear case with increasing excitation amplitude. Nevertheless, contrary to the previous case for the Aegion earthquake, for amplitude of 0.50g the values of the stiffness coefficient are not lower than they are for lower excitation amplitude, such as 0.30g. This can be explained by looking at the shear wave velocities calculated in the soil profile. For earthquake amplitude of 0.30g, the shear wave velocities at depths 0.5m, 2m, and 5m are 173m/s, 154m/s and 128m/s respectively. For the larger amplitude of 0.50g, the shear wave velocities are the same depths are 176m/s, 162m/s and 140m/s respectively. This indicates that the stiffness coefficient at the higher frequency range (dominated by the response at the upper soil layers) will be larger for the earthquake of the 0.50g amplitude. This contradictory phenomenon can be explained by the different frequency content of the signal which excites different resonant frequencies of the soil profile. The uppermost soil layers seem to be excited less by the strongest earthquake amplitude of 0.50g. On the other hand, the radiation damping coefficient is not affected by the different earthquake ground motion.

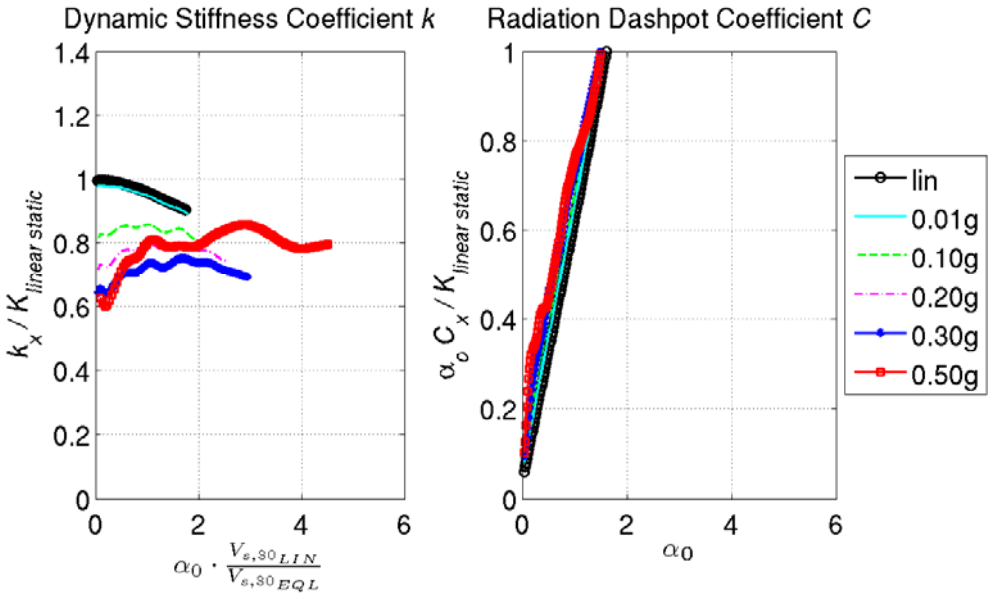

Figure 10. Horizontal dynamic stiffness and radiation dashpot coefficients for a homogeneous soil profile, with clay IP0 soil, initial shear wave velocity $V_{s,30,LIN}$=180m/s, subjected to the San Rocco earthquake record

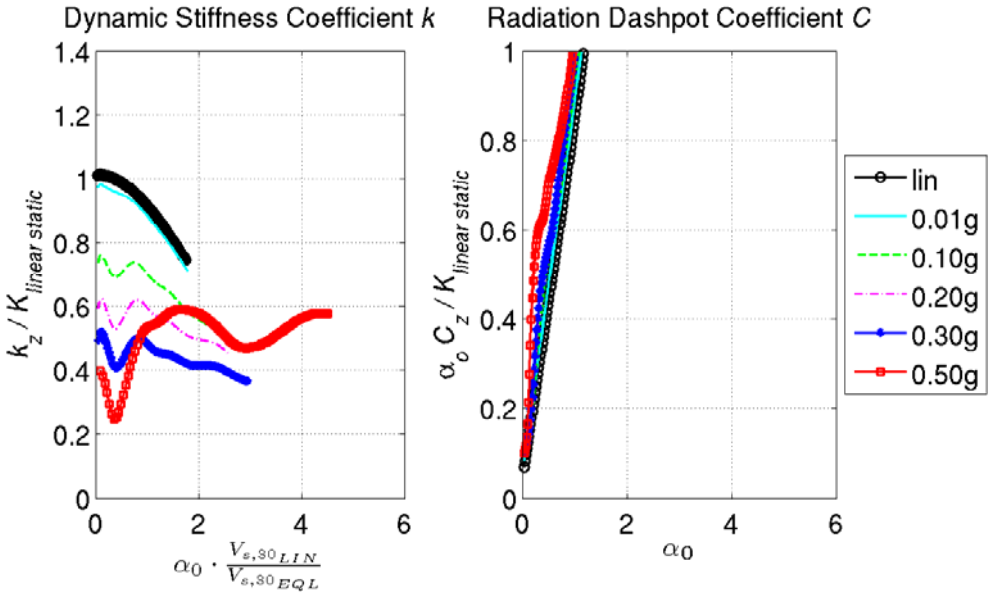

Figure 11. Vertical dynamic stiffness and radiation dashpot coefficients for a homogeneous soil profile, with clay IP0 soil, initial shear wave velocity $V_{s,30,LIN}$=180m/s, subjected to the San Rocco earthquake record

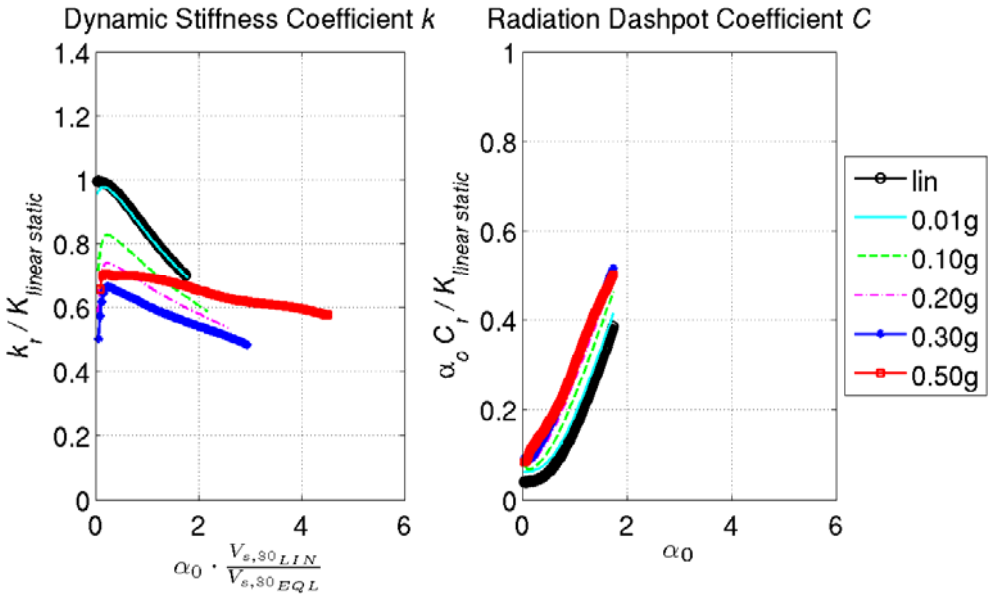

Figure 12. Rocking dynamic stiffness and radiation dashpot coefficients for a homogeneous soil profile, with clay IP0 soil, initial shear wave velocity $V_{s,30,LIN}$=180m/s, subjected to the San Rocco earthquake record

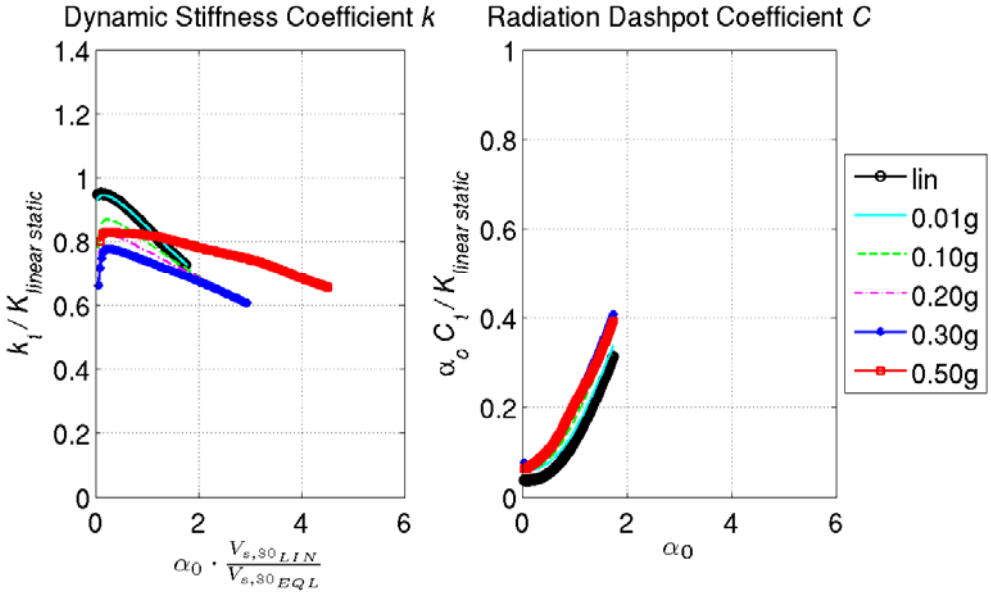

Figure 13. Torsional dynamic stiffness and radiation dashpot coefficients for a homogeneous soil profile, with clay IP0 soil, initial shear wave velocity $V_{s,30,LIN}$=180m/s, subjected to the San Rocco earthquake record

In the vertical mode (Figure 11) the same trend is observed for the dynamic stiffness coefficient response, not proportional to the excitation amplitude. While for amplitudes up to 0.30g the stiffness coefficient decreases from the linear case with increasing amplitude, for excitation at 0.50g the stiffness coefficient decreases less than it does for lower amplitudes. Besides, sharper valleys and flatter peaks also appear at the low frequency range, compared to the Aegion case shown before. The sharp drop of the stiffness coefficient for the amplitude 0.50g, at a dimensionless frequency $\alpha_0 \, c \, V_{s,30,LIN} / V_{s,30,EQL}$ around 0.5 is associated with the rapid increase of the vertical radiation damping at that frequency range. Attention should be made as it may seem that the dynamic stiffness coefficient attains larger values than the linear case in the higher frequency range larger than 2. This misconception arises from the fact that the dynamic stiffness coefficient is plotted against $\alpha_0 \, c \, V_{s,30,LIN} / V_{s,30,EQL}$, which shifts the represented values to the higher frequency range.

In the rocking and the torsional modes (Figure 12 and 13), the dynamic response of the footing is similar in trend as in the horizontal and vertical modes. The strongest amplitude of the earthquake record tends to decrease less the dynamic stiffness coefficient. Nonetheless, the dynamic stiffness coefficients of the rocking and torsional modes do not experience any resonance phenomena, as seen also in the previous cases for the Aegion earthquake record. They decrease monotonically with increasing frequency. The radiation dashpot coefficients increase with increasing amplitude of the motion, due to larger hysteretic material damping in the soil, and increase with increasing frequency at a rate similar to the linear elastic case. Small values of radiation damping are exhibited in the rocking and torsional modes of vibration.

CONCLUSIONS

A parametric analysis was conducted to demonstrate the effect of different input ground motion on the dynamic impedance functions, when nonlinear soil behavior is accounted. The nonlinear soil behavior was approximated by an equivalent linear procedure and the dynamic impedance functions of a typical footing resting on a typical soil profile were calculated and compared with the linear elastic soil case. The principal findings can be summarized as follows.

- The dynamic response of the footing for the nonlinear case depends on more parameters than in the linear case. The complexity of the linear problem is augmented in the nonlinear case by the influence of the shear wave velocity of the profile (it decreases in the nonlinear case), the soil material (characterized by the shear modulus reduction and damping curves) and the excitation amplitude and frequency content.
- The dynamic stiffness coefficient decreases from the linear case with increasing excitation amplitude.
- The dynamic stiffness coefficient for the initially homogeneous soil profile may increase, decrease, or become practically constant with increasing frequency. The response of the stiffness coefficient depends on the modification of the soil shear wave velocity due to the equivalent linear soil behavior. The shear wave velocity may indeed decrease significantly with increasing depth, contrary to the traditional increase, or stiffening, with increasing depth. Therefore, an increase of the stiffness coefficient with increasing frequency may be as well expected, since this inversion of the shear wave velocity may be encountered. Nevertheless, this phenomenon is produced only when there is a significant decrease of the shear wave velocity in the deeper soil layers, due to the equivalent linear soil behavior and its inherent deficiencies.
- In the nonlinear soil profile inhomogeneous soil layers are formed and, consequently, resonant frequencies of the soil appear as fluctuations of the dynamic stiffness coefficient at those frequencies. These undulations are of larger amplitude for the vertical and horizontal vibration modes, while they do not appear in the rocking and torsional modes. The larger fluctuations for the vertical mode are attributed to the deeper zone of influence of the normal stresses induced by the response of the footing to vertical loading.

- Depending on the individual characteristics of the input ground motion, different behavior may be observed for the stiffness coefficients, resulting from independent resonances of the exciting signal with the soil. These differences are filtered out with the averaging of the earthquake ground motions.
- The radiation dashpot coefficient is fairly dependent on the excitation amplitude. It increases from the linear case with increasing level of excitation mainly due to the increase of the hysteretic material damping in the soil.
- The radiation dashpot coefficient exhibits smooth undulations at the resonant frequencies of the newly formed inhomogeneous soil.

REFERENCES

CEN (2002) Eurocode 8, Comite Europeen de Normalisation, Prenorme ENV 1997-1

Dobry R., and Gazetas G. (1986) "Dynamic response of arbitrarily shaped foundations", Journal of Geotechnical Engineering Division – ASCE, Vol. 112, No. 2, pp. 109-135

Dobry R., Gazetas G., Stokoe II K.H. (1986) "Dynamic response of arbitrarily shaped foundations", Journal of Geotechnical Engineering Division – ASCE, Vol. 112, No. 2, pp. 136-154

Gazetas G. (1983) "Analysis of machine foundation vibrations: state of the art". Soil Dynamics and Earthquake Engineering, Vol. 2, No. 1, pp. 2-42

Gazetas G. (1991) "Formulas and charts for impedances of surface and embedded foundations", Journal of Geotechnical Engineering Division -- ASCE, Vol. 117, No. 9, pp. 1363-1381

Gazetas G. and Stokoe K.H. (1991) "Free vibration of embedded foundations: Theory versus experiment", Journal of Geotechnical Engineering Division - ASCE, Vol. 117, No. 9, pp. 1382-1401

Mylonakis G., Nikolaou S., Gazetas G. (2006) "Footings under seismic loading: Analysis and design issues with emphasis on bridge foundations", Soil Dynamics and Earthquake Engineering, Vol. 26, No. 9, pp. 824-853

Pecker A. (1997) Analytical formulae for the seismic bearing capacity of shallow strip foundations in Seismic Behavior of Ground and Geotechnical Structures, Balkema, Rotterdam, pp. 261-268

Pitilakis D. (2006) Soil-structure interaction modeling using equivalent linear soil behavior in the substructure method, Ph.D. Thesis presented in Ecole Centrale Paris, France

Sieffert J.-G., and Cevaer F. (1992) Manuel de fonction d'impedance, Ouest Editions/AFPS, Nantes, France

Veletsos A.S., Wei Y.T. (1971) "Lateral and rocking vibration of footings", Journal of Soils Mechanics and Foundation Division – ASCE, Vol. 97, No. SM9, pp. 1127-1248

Veletsos A.S., Verbic B. (1973) "Vibration of viscoelastic foundations", Earthquake Engineering and Structural Dynamics – ASCE, Vol. 2, pp. 87-102

Vucetic M. (1994) "Cyclic threshold shear strains in soils", Journal of Geotechnical Engineering Division – ASCE, Vol. 120, No. 12, pp. 2208-2228